JOURNAL OF GEOPHYSICAL RESEARCH, VOL. 102, NO. D24, PAGES 28,953–28,966, DECEMBER 26, 1997

Seasonal variation of carbon dioxide, water vapor, and energy exchanges of a boreal black spruce forest

P. G. Jarvis, J. M. Massheder, S. E. Hale, J. B. Moncrieff,
M. Rayment, and S. L. Scott

Institute of Ecology and Resource Management, University of Edinburgh, Edinburgh, Scotland

Abstract. Measurements of the fluxes of latent heat λE, sensible heat H, and CO_2 were made by eddy covariance in a boreal black spruce forest as part of the Boreal Ecosystem-Atmosphere Study (BOREAS) for 120 days through the growing season in 1994. BOREAS is a multiscale study in which satellite, airborne, stand-scale, and leaf-scale observations were made in relation to the major vegetation types [*Sellers et al.*, 1995]. The eddy covariance system comprised a sonic anemometer mounted 27 m above the forest, a system for transferring air rapidly and coherently to a closed path, infrared gas analyzer and a computer with the Edinburgh EdiSol software. Over the measurement period, closure of the energy balance on a 24 hour basis was good: $(H + \lambda E)/(R_n - G - B - S) = 0.97$. The midday Bowen ratio was typically in the range 1.0–2.5, with an average value of ~1.9 in the first Intensive Field Campaign (IFC1) and 1.3–1.4 in IFC2 and IFC3. Daily ecosystem evapotranspiration from moss, understory, and trees followed daily net radiation. Mean half-hourly net ecosystem flux followed photosynthetic photon flux density (PPFD) closely, reaching -9 μmol m^{-2} s^{-1} in June and August. The mean respiratory efflux on nights during which the atmosphere was well mixed ($u^* > 0.4$ m s^{-1}) reached 6 μmol m^{-2} s^{-1}. The PPFD-saturated biotic CO_2 assimilation reached 20 μmol m^{-2} s^{-1} and showed little response to air temperature or vapor pressure deficit (VPD). Storage of CO_2 in the air column at night did not account adequately for respiration on stable nights, so nighttime efflux was modeled for periods when $u^* < 0.4$ m s^{-1}. There was a net gain of CO_2 on most of the 120 days, but on 31 days of high temperature or low PPFD there was a net carbon loss. High PPFD promoted influx of CO_2 by the foliage, whereas high temperatures reduced net CO_2 influx through high respiration rates by the roots and soil microorganisms, leading to lower net uptake at high PPFD. Over the 120 day period, 95 g m^{-2} of C were stored (an average of 0.8 g m^{-2} d^{-1}), and 237 mm of water evaporated (an average of 2 mm d^{-1}).

Introduction

The boreal forest biome is very extensive, occupying about 17% of the global vegetated land surface and thus may be an important driver of global weather and climate. The exchanges of radiation and sensible and latent heat at the surface are likely to lead to significant feedbacks between processes at the surface and properties of the atmosphere [*Sellers et al.*, 1995].

In addition, the biome may make a significant contribution to the global carbon budget, with further consequences for atmospheric properties. The best current estimates of the global carbon balance indicate that of the 7.5–8 Pg of carbon that is put into the atmosphere each year from anthropogenic activities, between 3 and 4 Pg remain in the atmosphere, 1.5–2 Pg may be transferred to the oceans [*Keeling et al.*, 1996], leaving between 2 and 3 Pg unaccounted for. Circumstantial evidence, largely based on inverse modeling of the global network, flask sample data for $[CO_2]$, ^{13}C, and ^{18}O in CO_2, suggests that major sinks for this carbon may lie in the middle and high latitudes that straddle the northern temperate and boreal forests of the world [*Conway et al.*, 1994; *Ciais et al.*, 1995; *Denning et al.*, 1995; *Francey et al.*, 1995].

Copyright 1997 by the American Geophysical Union.

Paper number 97JD01176.
0148-0227/97/97JD-01176$09.00

The Boreal Ecosystem-Atmosphere Study (BOREAS) was designed to address these two issues (among others) [*Sellers et al.*, 1995]. BOREAS is a multiscale investigation in which satellite, airborne, stand-scale and leaf and soil-scale observations have been made in relation to the major vegetation types in the boreal forest region of central Canada. In this region the boreal forest biome consists of extensive areas of fens, lakes, and forests that are largely composed of black spruce (*Picea mariana*), jack pine (*Pinus banksiana*), tamarack (*Larix laricina*), and aspen (*Poulus tremuloides*). Of these, the dominant vegetation type is black spruce, extensive stands of which occupy approximately 50% of the region lying between Prince Albert in the south and Thompson in the north [*Ogunjemiyo et al.*, this issue].

The specific objectives of the investigation described here during the 1994 campaign were to determine the net ecosystem exchanges of radiation, sensible and latent heat (water vapor), and carbon dioxide of an extensive, typical stand of black spruce in the southern study area of BOREAS, with the aims of assessing possible interactions between evaporation from the forest and the atmosphere and, in particular, determining whether the stand of black spruce was a significant sink for atmospheric carbon. Parallel studies on neighboring sites were in progress over the same period [e.g., *Baldocchi et al.*, this issue, and 1997].

Site Characteristics

The site lies in the southern, mixed forest zone of the Canadian boreal forest about 100 km north of Prince Albert in the province of Saskatchewan (53.987°N, 105.118°W). The landscape in the region is predominantly flat and covered with pure and mixed stands of black and white spruce, jack pine, aspen, fen, and lakes.

Measurements were made in an extensive forest of old black spruce (OBS) (*Picea mariana* (Mill.) BSP). From the micrometeorological tower there was a uniform fetch of at least 1200 m in all directions, apart from a gash in the forest to the northeast created by the electrical power utility when bringing electricity to the site in 1993. The terrain around the site was essentially flat, with slight rises and falls of less than 1% and a total height variation of less than 1 m. The substratum was peat overlying glacial drift with an elevated water table so that the surface was generally wet. For this reason access to the measurement area was by a 2 km boardwalk.

Measurements began in the early spring of 1994 and continued to the autumn. A near-continuous set of half-hourly flux data were obtained over 120 days from May 23 (day of year 143) to September 21 (day 264). When measurements began in May, there was ice in the soil profile between about 25 and 40 cm and snow had fallen recently. When measurements ceased in the autumn, the first frosts had already occurred. Compact airborne spectrographic imager (CASI) images of the area (J. Miller, personal communication, 1996) show that the tower is at the center of a relatively dense stand of well-grown trees that extends for 300 m in all directions. Similar areas extend for up to 1 km to the north (320°–20°) and to the south (140°–220°). Elsewhere, the forest is a mosaic of similar patches of relatively well-grown trees and patches, 200–300 m across, of more poorly drained, slightly lower lying ground where the trees are smaller and the stand is more open.

The tree stand was largely black spruce with ~10% tamarack (*Larix laricina* (Du Roi) K. Koch), occasional jack pine (*Pinus banksiana* Lamb.), and balsam poplar (*Populus balsamifera* L.). The height of the stand was 10–11 m, with the occasional tamarack reaching 16 m. There were ~5900 stems per hectare ranging in diameter (dbh) from 3 to 20 cm with a modal diameter of 8 cm and basal area of 30 m^2 ha^{-1}. The stand was fairly uniform in age (~115 years), probably because it developed after a fire. Projected leaf area index was highly variable across the site, averaging 4.5 [*Chen et al.*, this issue; *Gower et al.*, this issue]. The live crowns of the black spruce trees were up to 6 m in length but were exceptionally narrow, generally being less than 2.5 m in diameter with highly aggregated foliage densely packed in a small volume. Thus, despite the leaf area index of over 4, there were appreciable gaps among the trees. The annual total above and below ground net primary production is 2.7 t C ha^{-1} [*Gower et al.*, this issue].

There was a sparse understory with some low shrubs reaching a height of ~1.5 m (e.g., *Ledum groenlandicum*, *Vaccinium uliginosum*, *Potentilla fructicosa*, *Rubus idaeus*, *Rosa acicularis*, *Lonicera dioica*, *Betula glandulosa*, *B. glandulifera*, *Salix* spp.), a varied mixed tall herb community, particularly in the open areas (e.g., *Mertensia paniculata*, *Geum aleppicum*, *Solidago canadensis*, *S. spathulata*, *Aster puniceus*, *Petasites palmatus*, *P. sagittatus*, *Potentilla palustris*, *Gallium boreale*, *Lillium philadelphicum*, *Platanthera hyperborea*, *Spiranthes romanzoffiana*, *Equisetum sylvaticum*), and occasional dwarf shrubs (e.g., *Vaccinium vitis-idaea*, *Andromeda polifolia*, *Kalmia polifolia*, *Cornus canadensis*).

The ground had a hummock-hollow microtopography in the wetter areas, with hummocks of *Sphagnum* spp. and occasional surface water in the hollows. This graded into feather mosses (e.g., *Hylocomium splendens*, *Pleurozium schreberi*) and lichens (*Cladina* sp.) in the drier areas.

Methods

A 25 m tower and an associated heated cabin with 240 and 110 V ac line power, 20 m from the foot of the tower, were provided by the BOREAS project management. A weather station and the micrometeorological flux measuring equipment were mounted on the tower: data recording equipment, computers, and some measuring systems were installed in the cabin.

Weather Station

A weather station was maintained throughout the field season to provide comprehensive meteorological measurements. All data were recorded as half-hourly averages on a datalogger (21X, Campbell Scientific (UK) Ltd., Shepshed, England). All instrumentation, unless stated otherwise, was mounted at the top of the tower (at about 26 m). Temperature and humidity were measured using a shielded thermistor and capacitance humidity probe (Campbell Scientific (UK) Ltd.), and in addition, wet and dry bulb temperatures were obtained using a ventilated psychrometer, with a platinum resistance thermometer and a thermocouple. A cup anemometer and wind vane (Vector Instruments, Rhyl, Wales) measured wind speed and direction, respectively. Two net radiometers (Q-6, REBS, Seattle, Washington) projected on booms from the southern face of the tower at a height of 18 m, and the average of the two readings was taken. Two solarimeters (CM3, Kipp & Zonen, Delft, The Netherlands) were also mounted on these booms, measuring incoming and reflected solar radiation. Incoming solar radiation was also measured using a pyranometer (LI-COR Inc., Lincoln, Nebraska). Photosynthetic photon flux density (PPFD) was measured with a quantum sensor (LI-COR Inc.), and rainfall was measured using a tipping bucket rain gauge (Cassella, London). In addition to these above-canopy measurements, a net radiometer (Q-7, REBS) was positioned below the canopy, at a height of 2 m above the ground.

Soil heat flux was measured using an array of seven soil heat flux plates (HFT-3, Campbell Scientific (UK) Ltd.). These were buried about 2 cm below the soil surface in a range of situations, to represent the heterogeneity of the environment. A soil temperature probe measured a profile of soil temperatures with thermocouples at depths of 2.5, 5, 10, 20, and 50 cm, referenced to the temperature at 1 m.

Eddy Covariance Measurements of Fluxes

During the 1980s, Denmead and his colleagues experimented with pumping air from close to a sonic anemometer down a long tube to a conventional, closed path, infrared gas analyzer to measure CO_2 fluxes over forests [*Denmead and Bradley*, 1989]. Subsequent advances in closed-path gas analyzer technology have led to the development of this as a practical approach to the long-term measurement of fluxes [*Wofsy et al.*, 1993; *Goulden et al.*, 1996b].

Fluxes of momentum, sensible heat, water vapor, and CO_2

were measured using the University of Edinburgh EdiSol system [*Moncrieff et al.*, 1997]. A three-dimensional sonic anemometer (Solent, Gill Instruments Ltd., Lymington, England) was mounted 2.6 m above the top platform on a vertical pole on the SW corner of the tower at a height of 27 m. The air was ducted by heated tube (Dekabon 13, Samual Moore, Ohio) at 6 dm^3 min^{-1} from close to the anemometer to an infrared gas analyzer (LI-6262, LI-COR Inc.) in a custom-built enclosure at the foot of the tower. The enclosure also contained pump, temperature and pressure transducers, tube heating control, laptop, and other accessories.

EdiSol collects 20 readings of wind speed components, speed of sound, CO_2 concentration c, and water vapor concentration q every second from the Solent. A digital recursive running mean with a constant of 200 s is subtracted from each of the values of these variables to give the fluctuations from the mean and the covariances calculated, $w'T'$, $w'c'$, and $w'q'$. The latter two covariances are stored in a buffer to allow for the time taken for the air to travel down the sample tube. At the end of a flux-averaging period (usually 30 min), several further calculations are done. Coordinate rotation orientates the wind velocity components relative to the local streamlines, eliminating contamination of the vertical fluxes by horizontal wind. Correlations between vertical wind speed fluctuation, w' and c' and q' with various lags, are calculated. The extreme values give the travel time down the tube for each variable. These calculated lags are then used to select the correct covariance from the buffer with which to calculate the fluxes. Fluctuations in the density of air caused by varying heat and water content can cause errors in the measurement of CO_2 and water vapor flux [*Webb et al.*, 1980]. However, corrections for this are not required when using the LI-6262 closed-path gas analyzer; the temperature fluctuations are damped as the air travels down the tube and comes to a constant temperature in the analyzer, and the effects of water vapor are eliminated by the software in the analyzer, which calculates the CO_2 concentration in dry air [*Leuning and Judd*, 1996].

Discrete samples are taken of a continuously varying fluid. Some attenuation of the high-frequency component occurs during flow down the tube and, furthermore, the gas analyzer has a limited frequency response. Consequently, a part of the high-frequency component of the flux is missing from the measurement. To correct for this loss, all primary data were collected at regular intervals, and the cospectrum for both water vapor and CO_2 flux calculated, and compared against the similar cospectrum for heat flux measured at the sonic anemometer over the same period. Based on the differences in the cospectra, separate corrections for loss of signal, typically 15%, were then applied to the previously calculated water vapor and CO_2 fluxes [*Moncrieff et al.*, 1997].

Canopy Storage Fluxes

Flux measurements above the canopy give the net exchange between the ecosystem below and the atmosphere over the period of integration, i.e., the "net ecosystem flux." For any scalar, this flux is the algebraic sum of a number of fluxes within the system, including a flux in and out of storage within the air column below the measuring height. Over a day or more, the change in storage of sensible heat, water vapor, and CO_2 is very small, but over short periods of time, the storage flux may be very large in some conditions, so that it is necessary to measure it to be able to evaluate the total biotic flux during a particular period. Estimates of the change in storage of sensible heat and water vapor in the air column were very small and not calculated regularly. An estimate of change in heat storage in the trees was based on measurements of wood temperature in three trees at two depths at heights of ~1.5 and 6 m above the ground.

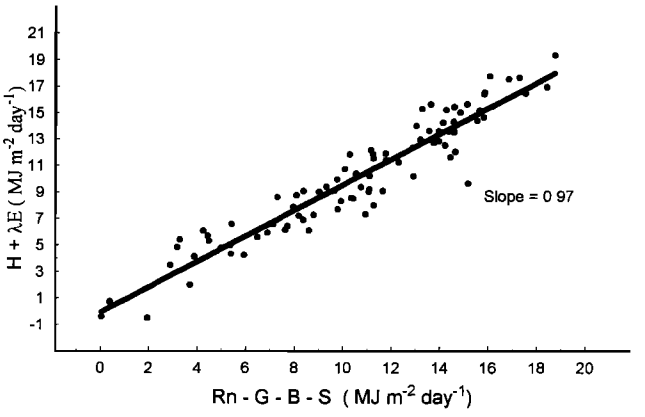

Figure 1. Mean daily energy balance of the black spruce stand in the BOREAS southern study area for the measurement period May 23 (day 143) to September 21 (day 264). The measured eddy fluxes of sensible heat H and latent heat λE are plotted against net radiation R_n less the energy storage terms. Each point represents the total energy exchanges over a 24 hour period. The line passes through the origin with a slope of 0.97.

Under stable atmospheric conditions in which there is limited ecosystem-atmosphere exchange, the eddy covariance system may measure little or no net exchange of CO_2 (depending on the height of the inversion layer), although the respiratory efflux of CO_2 from soil and biomass continues unabated. The CO_2 accumulated below the eddy covariance sensor may be detected later as it is flushed from the canopy by the onset of turbulent exchange or it may, in part, be reassimilated by canopy photosynthesis, during the early morning as the sun rises [*Goulden et al.*, 1996a, b; *Grace et al.*, 1996]. In either case, the flux in and out of storage needs to be measured, as well as

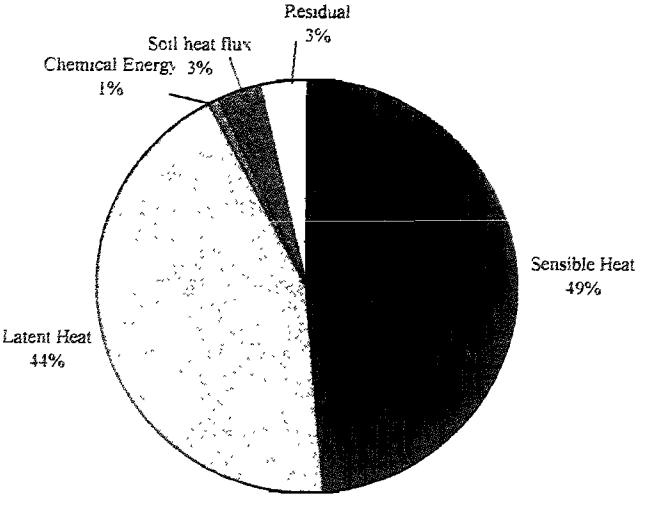

Figure 2. Partitioning of the total net radiation flux density over the entire growing season of 120 days from May 23 (day 143) to September 21 (day 264).

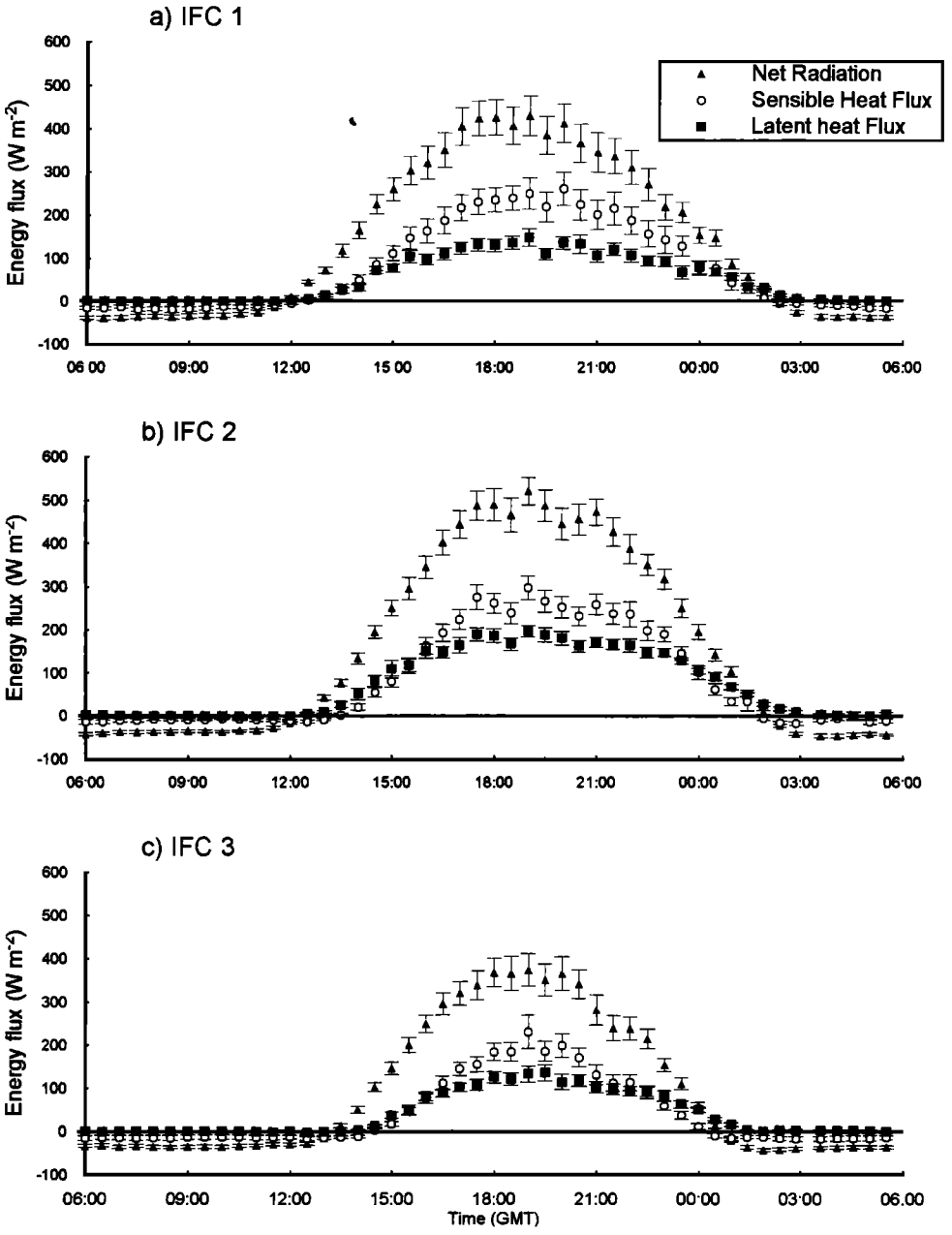

Figure 3. Average daily course of net radiation and sensible and latent heat flux densities for each intensive field campaign (IFC). IFC1 extended from May 24 (day 144) to June 16 (day 167); IFC2 from July 17 (day 198) to August 8 (day 220); IFC3 from August 30 (day 242) to September 19 (day 262). Each point is the value of the half-hourly average of the flux before the time shown on every day in the IFC. The maximum number of missing flux days in any IFC is two; a small number of hours is also missing from among the days included because of recalibration of the gas analyzer and changing filters. The error bars show ± 1 standard error.

the eddy flux, to evaluate the correct biotic flux in any half-hour period.

Assuming horizontal homogeneity, the amount of CO_2 in the canopy volume was calculated by measuring the profile of CO_2 concentration of the air within the canopy near the tower and integrating over the volume of the vertical column.

Air samples were drawn continuously from five heights, 27, 12, 6, 3, and 1.5 m (corresponding very approximately to $2h$, h, $h/2$, $h/4$, and $h/8$, where h is the mean canopy height), through 4 mm internal diameter nylon tubes, at a flow rate of 1 dm^3 min^{-1}. The sampling end of each tube projected downward and was wrapped with gauze and covered with an inverted funnel to prevent intake of insects and/or water. Immediately downstream of this was a Whatman particulate filter. A solenoid-based switching system sampled air from each line in turn and diverted 0.5 dm^3 min^{-1} of this air to an infrared gas analyzer (ADC 225 Mk iii, Analytical Development Company Ltd., Hoddesdon, England) to measure CO_2 concentration. In addition, air purged of CO_2 was sampled periodically to provide a zero reference. Air from each line was passed through the analyzer for 2 min, the first minute of which was ignored to ensure no contamination from the previous sample. Then the

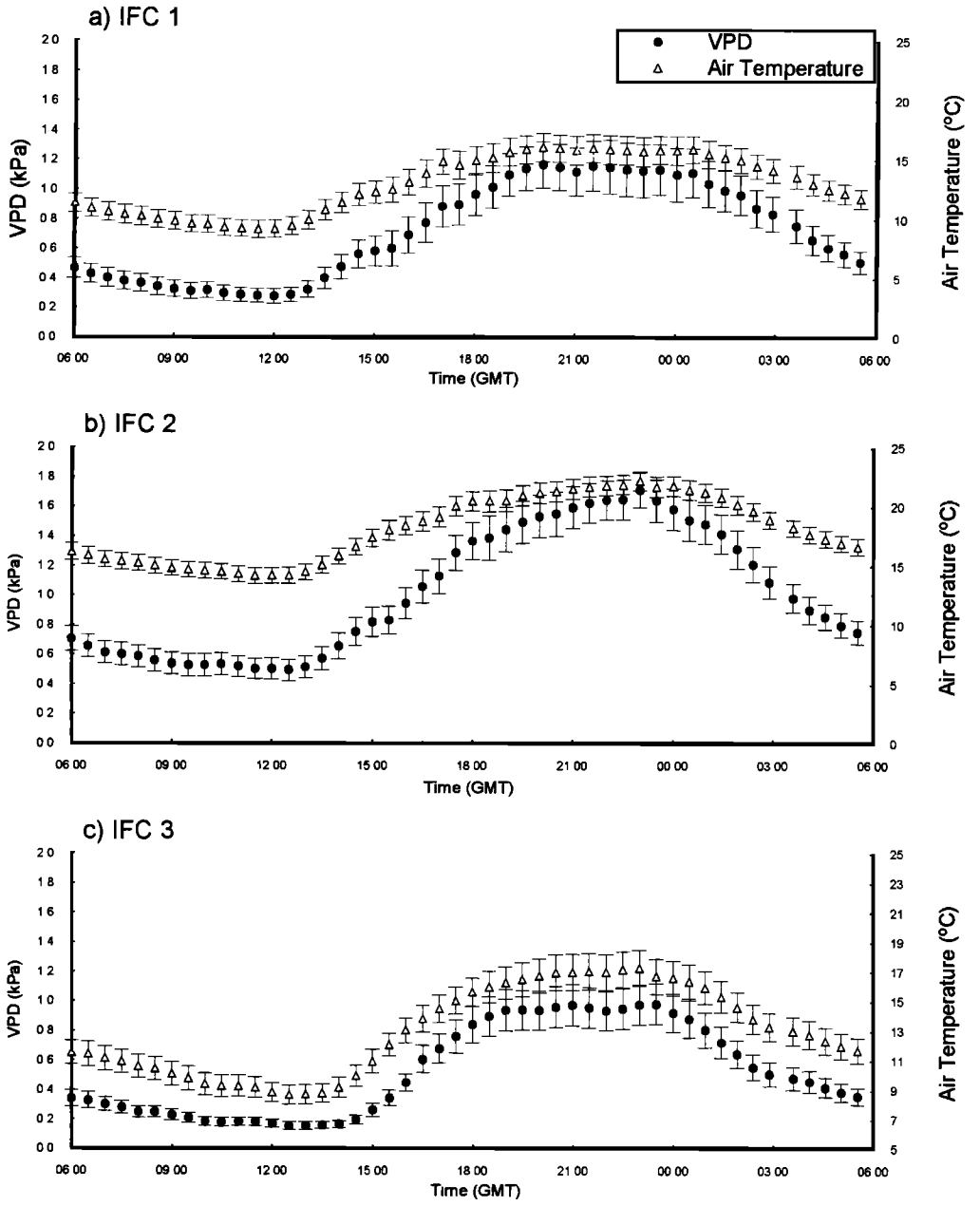

Figure 4. Average daily course of air temperature and water vapor pressure deficit at a height of 26 m during the three IFCs. Other details are as given for Figure 3.

average concentration for the second minute was recorded with a data logger (CR21X, Campbell Scientific (UK) Ltd.). Thus each of five heights in the canopy was sampled for 1 min every 10 min. Half-hourly means were calculated for the CO_2 concentration at each height, and the total amount of CO_2 in a vertical column of air 1 m^2 in cross-sectional area and 27 m high was calculated according to the formula

$$\sum_{n=1}^{n=5} (h_n - h_{n-1}) \left(\frac{|CO_2|_n + |CO_2|_{n-1}}{2} \right) \left(\frac{1000}{V_{Mair}} \right)$$

where $n = 1, \ldots, 5$ are the sample height numbers and h is the sample height in meters. $|CO_2|$ is the CO_2 concentration in μmol mol^{-1} and V_{Mair} is the molar volume of air, 22.4 dm^3 mol^{-1} at STP. It was assumed that the concentration measured at the lowest sampling point of 1.5 m was representative of the concentration between that height and the ground surface.

Instrument Calibration

The infrared gas analyzers were calibrated for CO_2 against secondary reference CO_2 gas bottles (Praxair Products Inc., Saskatoon, Canada), which were kept on site and had been recalibrated against the BOREAS primary standard CO_2 reference bottles to within 1 μmol mol^{-1}. The analyzers were calibrated for humidity against a constant dew-point source (LI-610 Humidity Calibrator, LI-COR Inc.). The eddy flux infrared gas analyzer was calibrated approximately every 1–2 weeks, as in practice, its gain and zero offset were steady over this period.

The net radiometers were cross-calibrated against BOREAS

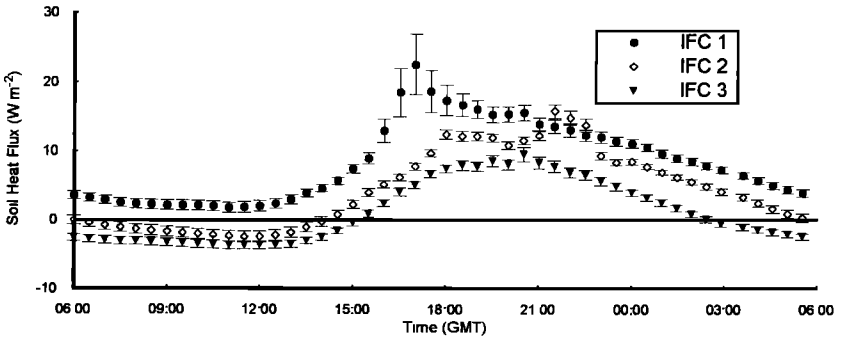

Figure 5. Average daily course of soil heat flux during the three IFCs. There were four heat flux plates during IFC1 and seven during IFC2 and IFC3. Other details are as given with Figure 3.

project reference net radiometers (E. A. Smith, personal communication, 1996). The solid-state Skye humidity sensor was cross checked against the wet and dry bulb psychrometer at regular intervals and used to replace missing psychrometer data. For all other weather station and radiation instruments, the manufacturers' calibrations were assumed. All quantum sensors were intercompared and referred back to one recently calibrated.

Measurement Protocol

Eddy covariance flux measurements at 27 m were made continuously in 1994 from the start of the first Intensive Field Campaign (IFC1), May 23 (day 143), to the finish of IFC3, September 21 (day 264). Throughout this period, the weather station was operated continuously, and the CO_2 profile system was operated for 114 days.

In addition, soil CO_2 efflux was measured at regular intervals with two systems that were rotated around 10 previously installed rings near the flux tower at approximately 2-day intervals. Stem CO_2 efflux was similarly measured on a number of trees near the tower. Collaboration with M. Lavigne provided measurements at regular intervals on a large number of black spruce trees on a site 2 km to the NNE. Photosynthesis, transpiration, and stomatal conductance were measured in two branch bags, one in the upper crown, the other in the lower crown, on the southern side of a median-sized tree in the same general area around the flux tower from August 30 (day 242) to September 15 (day 256). (The same bags had earlier been used on the jack pine site and were loaned to us by B. Saugier of the University of Paris-Sud). Results of these studies are referred to here, but they are not reported in detail.

Shorter studies was made of turbulence above and within the tree canopy using a profile of eight sigma-T sensors, two additional sonic anemometers, and two open-path water vapor analyzers and of acclimation of photosynthetic capacity with depth in the canopy in relation to recently absorbed radiation. The results of these studies will not be referred to here.

Results and Discussion

Stand Energy Balance

The energy balance of the stand can be expressed as

$$R_n = H + \lambda E + G + B + S \quad (1)$$

where R_n is net radiation, H is sensible heat flux, λE is latent heat flux, G is soil heat flux, B is biochemical energy stored by photosynthesis, and S is heat storage within the stand. Figure 1 shows the daily energy balance as $(H + \lambda E)$ plotted against $(R_n - G - B - S)$. This treatment gives a check on the

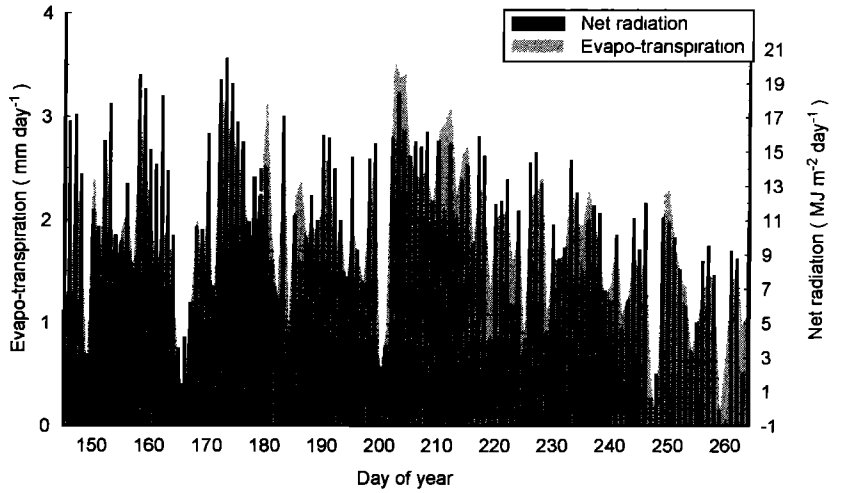

Figure 6. Seasonal course of daily integrated evaporation flux density and net radiation flux density for the 120 days from May 23 (day 143) to September 21 (day 264). Each column represents the total flux density integrated over 24 hours.

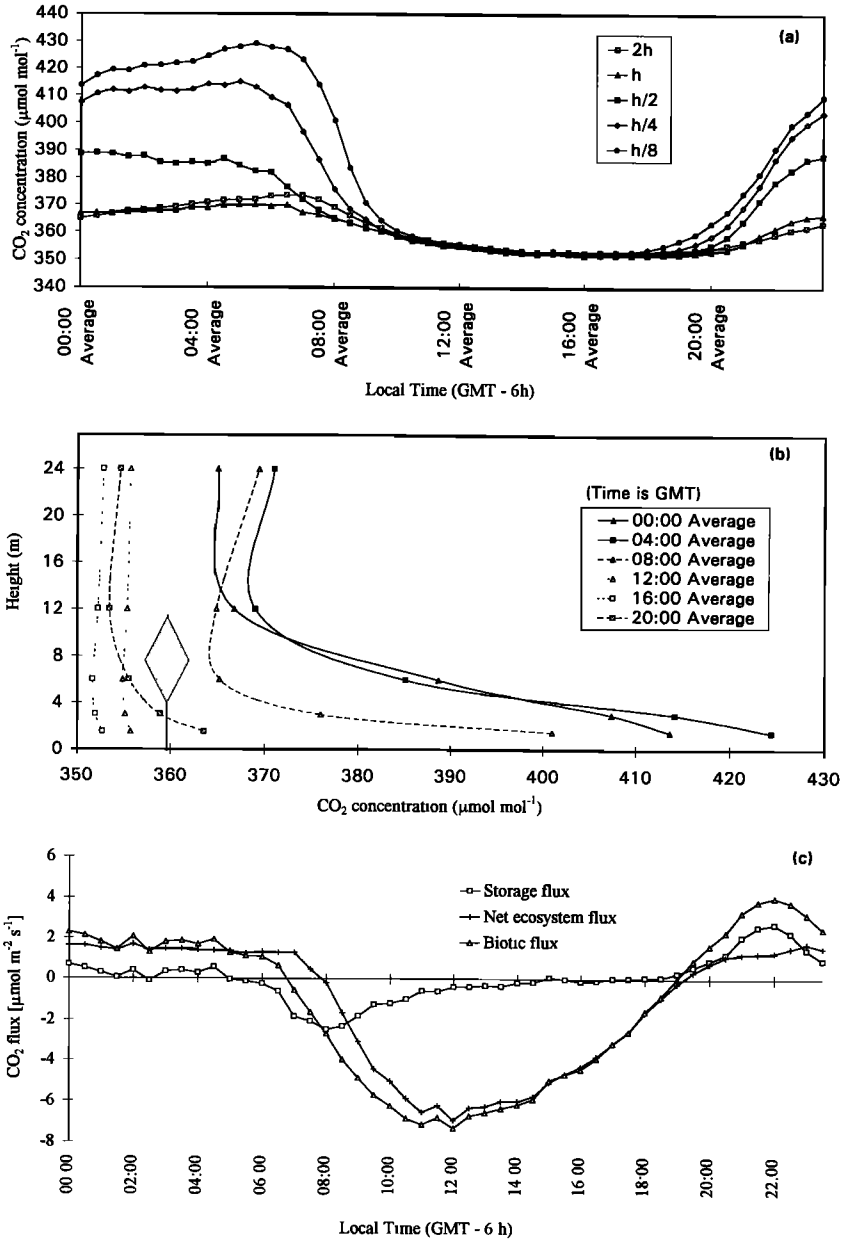

Figure 7. (a) Mean daily diurnal CO_2 concentrations at five heights between the eddy covariance sensor and the ground for the 114 days of profile measurements, (b) the same data plotted as vertical profiles, and (c) the mean daily diurnal storage flux, net ecosystem flux, and algebraic sum of the two, the ecosystem biotic flux.

sensible and latent heat fluxes as measured by eddy covariance against independently measured variables. The slope of 0.97 shows good agreement between measurements. Figure 2 shows the partitioning of energy among the components on the right-hand side of (1) over the period of measurements. Only 1% of the net radiation is stored by photosynthesis, whereas 93% of the net radiation is lost by sensible or latent heat flux. These proportions are quite typical of coniferous forest [*Jarvis et al.*, 1976]. The combined heat storage by the soil and vegetation of ~5% shows that over the period of measurements the stand was warming. Measurements were started when much of the soil was still partly frozen and some ice was still to be found in the soil profile in late June. Soil temperature at a depth of 1 m did not start to fall again until the beginning of September.

Diurnal Energy Balance

Figure 3 shows the average partitioning of available energy into sensible and latent heat flux during each of the three IFCs. Similar data are available for the inter-IFC periods but are not shown graphically. The average midday Bowen ratio was ~1.9 in IFC1, 1.6 in the period between IFC1 and IFC2, and 1.3–1.4 in IFC2, the following period and IFC3. While the hour to hour and day to day variability of the fluxes was broadly similar from the start of IFC1 up to the start of IFC3, the variability of the sensible heat flux on an hourly and a daily basis was much larger in IFC3. On some particular days of high midday temperature and vapor pressure deficit (VPD), midday Bowen ratios reached values of up to 3. These values of average

Bowen ratio in the range 1.3–1.9 are quite typical of earlier reported values for spruce forests that are not short of water [*Jarvis et al.*, 1976]. The magnitude of the Bowen ratio depends in part on the surface conductance but also on the ratio of atmospheric VPD to net radiation (i.e., the so-called climatic or isothermal resistance of *Monteith* [1965]), and the larger values (>2) in the literature for coniferous forests have tended to come from regions with oceanic climates and relatively small summer VPDs, whereas smaller values (<1) have been found in coniferous forests in more continental climates with larger seasonal VPDs [*Jarvis et al.*, 1976]. While further analysis of the data is required, it seems likely the high Bowen ratios in IFC1 can be largely attributed to the low VPDs then, possibly exacerbated by the cold soil with temperatures close to zero Celsius. The fall in Bowen ratio between IFCs 1 and 2 probably reflects the 50% increase in average atmospheric VPD (Figure 4), possibly augmented by the seasonal rise in soil temperature. While the average Bowen ratio remains low in September when the average midday VPD has fallen back to less than 1 kPa, the maximum soil temperatures which occur then, together with some drying of the top 15 cm of the soil (so that it is no longer waterlogged), provide the best conditions for water uptake by the tree roots at any time of the year.

The smaller energy fluxes are not shown in Figure 3 because they lie virtually on the zero line with the scale used. Figure 5, however, shows that the mean daily soil heat fluxes declined through the period from a morning peak of about 20 W m^{-2} in IFC1 to an afternoon peak of about 10 W m^{-2} in IFC3. Because of local heterogeneity on the forest floor and the small number of sensors, the absolute size of the fluxes must be regarded with caution, but the fall in soil heat flux as the season progressed is as expected. It is, however, noteworthy that there was still a significant heat flux into the soil in September.

Seasonal Evapotranspiration

Figure 6 shows the progression of daily total water loss by evaporation through the summer. It is noteworthy that evaporation rates were already high at the start of IFC1 in late May. While there was substantial variation from day to day, the overall pattern is broadly dome shaped, with maximum daily rates during IFC2 in July. The days that depart from this general trend with very low rates of evaporation are days of extreme cloudiness or with significant precipitation, as shown by the coincident low net radiation fluxes. While there are insufficient data as yet available from 1994 to partition the total evaporation between transpiration from the trees and understory shrubs and evaporation from the herbaceous and moss ground flora, data more recently obtained suggest that about $\frac{1}{4}$ of the total evapotranspiration may come from the ground flora when it is moist.

CO_2 Storage Flux

CO_2 concentrations within the canopy increased markedly at night, particularly at the lower levels (Figure 7a). The increase was largest, occasionally exceeding 600 μmol mol^{-1}, on nights with stable atmospheric conditions and temperature inversions. The nighttime increase was followed by a rapid return to ambient CO_2 concentrations early in the day. The same data are plotted as vertical profiles in Figure 7b.

The need to correct the net ecosystem flux for the storage component to give the biotic flux is most evident during the early morning, after sunrise but before the onset of turbulent mixing between the canopy volume and the atmosphere. Figure 7b shows that at this time the CO_2 concentrations measured within the canopy were drawn down to concentrations lower than those measured at 0200 local time (0800 profile), indicating that photosynthesis was reassimilating some of the CO_2 released by nighttime respiration. Because this CO_2 was retained within the canopy volume and not exchanged with the atmosphere, this early-morning photosynthesis was not detected by the eddy covariance sensor. Making corrections to the eddy covariance data for the storage flux shows that the biotic components of the ecosystem were a net sink for CO_2 more than 1 hour earlier than is apparent from the eddy covariance data alone (Figure 7c). Similarly, Figure 7c shows that the nighttime respiratory efflux of CO_2 from the forest floor and standing biomass was considerably underestimated by the eddy covariance data alone, particularly during the early evening, since at that time the temperatures of the soil and wood were still relatively high, resulting in the efflux of large amounts of CO_2 which were not exchanged with the atmosphere.

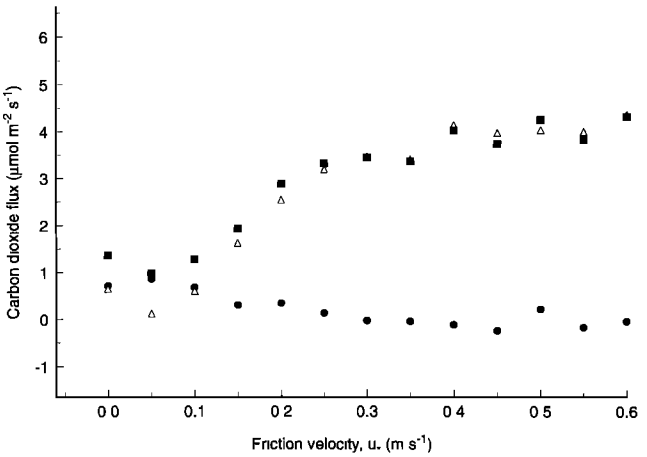

Figure 8. Mean nighttime storage flux (circles), net ecosystem flux (triangles), and sum of the two, the ecosystem biotic flux (squares), in relation to u^*. The half-hourly flux data have been averaged in classes of $0.05u^*$ over the entire measurement period.

To estimate this loss of flux at night, we have plotted the flux into storage in the air column and the net ecosystem flux against u^* in Figure 8. We have used almost all the nighttime data averaged across similar half-hour periods during the 120 days for this, binned into classes of $0.05u^*$. A statistical test showed no significant correlation between u^* and air temperature.

Figure 8 shows that the calculated flux into storage did not adequately compensate for the loss of eddy flux during nights with stable conditions and strong temperature inversions as found by others [e.g., *Goulden*, 1996a, b]. Consequently, we have modeled the nighttime CO_2 fluxes. A relationship was established between the measured nighttime eddy flux and soil temperature at a depth of 25 mm for unstable nights with $u^* > 0.4$ m s^{-1}, and this relationship was then used to calculate the nighttime CO_2 efflux for each half-hour period on nights when $u^* < 0.4$ m s^{-1}. There was considerable scatter in this relationship but no evidence of any systematic change through the growing season.

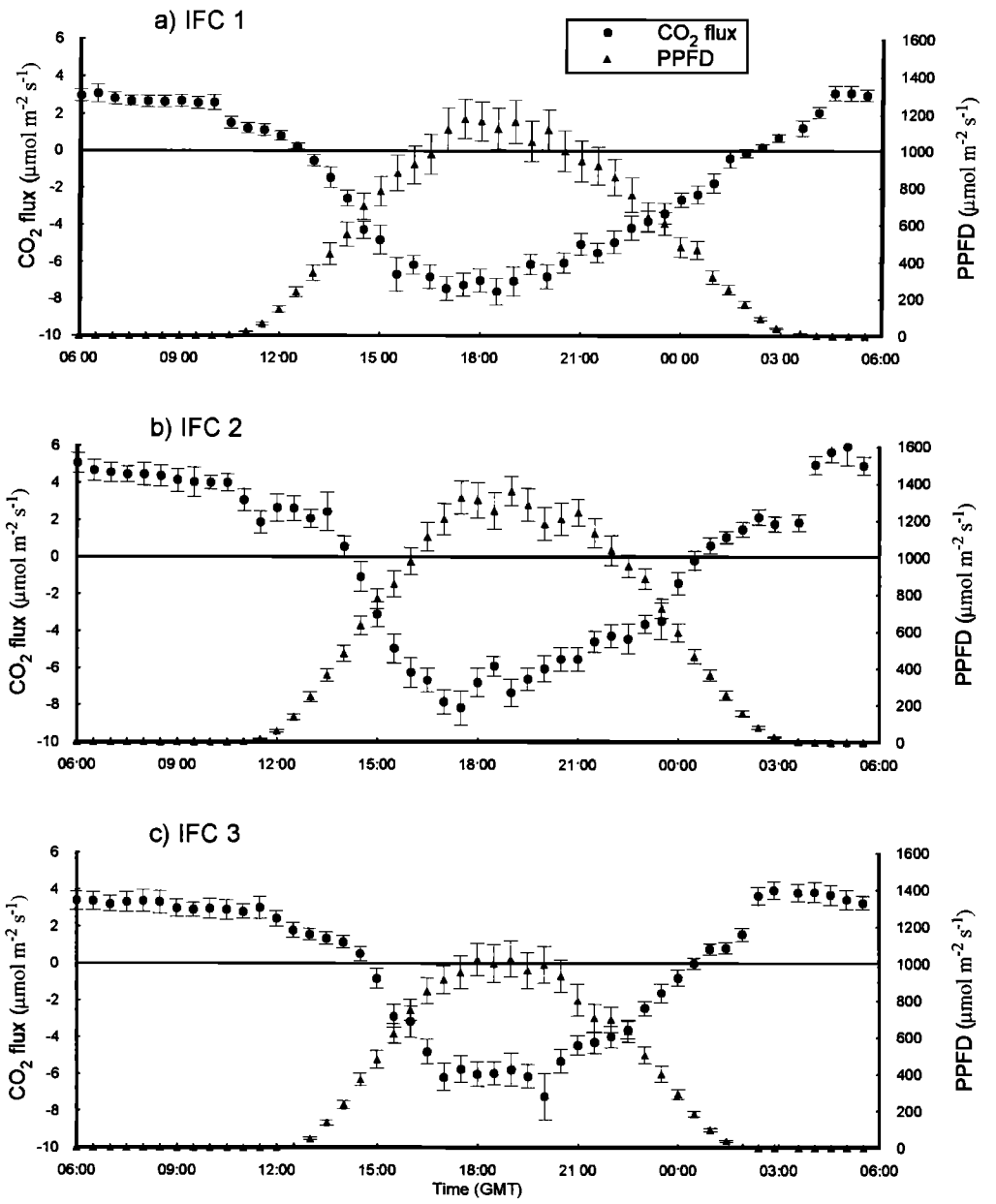

Figure 9. Average daily course of net ecosystem carbon dioxide flux density and photosynthetic photon flux density (PPFD) for each IFC. Other details are as given in Figure 3.

Diurnal Net Ecosystem Biotic CO_2 Flux

The average daily diurnal CO_2 flux for the three IFCs is shown in Figure 9. Similar data exist for the periods between the IFCs. The maximum average midday net influxes were about −7, −9, −8, −9, and −6 μmol m^{-2} s^{-1} for the sequence of periods from IFC1 to IFC3. Average nighttime effluxes resulting from respiration were ~3 μmol m^{-2} s^{-1} in IFC 1 and 3 but reached 6 in IFC2. Some individual half-hour fluxes greatly exceeded the average in particularly favorable conditions, and net influxes of −15 μmol m^{-2} s^{-1} were measured on a number of occasions (Figure 10). More analysis of the data for individual days is needed, but the highest rates of influx were generally recorded on overcast days of high PPFD.

Scatter diagrams of net ecosystem flux during unstable daylight conditions, shows a strong dependence of CO_2 influx on PPFD (Figure 10a). There is a large amount of scatter, as temperature and VPD were both highly variable. Ecosystem PPFD saturation was at about 1000 μmol m^{-2} s^{-1}, and the compensation PPFD at about 200 μmol m^{-2} s^{-1}. Figure 10b shows a strong reduction of net ecosystem flux at VPDs larger than 1 kPa, and there is an apparent optimum temperature for net ecosystem flux at about 16°C. To a considerable extent, PPFD, temperature, and VPD are correlated: high temperatures and VPDs occur on bright sunny days of high PPFD. Most important, the respiratory effluxes of CO_2 from the tree stems and soil are strongly temperature dependent. The measurements made of CO_2 efflux from the ground with chambers have demonstrated an exponentially increasing response to temperature with a median value of 3.2 μmol m^{-2} s^{-1} at 10°C and a median exponent of 0.70 (i.e., a doubling of the flux for a 10°C rise in temperature) [see *Rayment and Jarvis*, this issue].

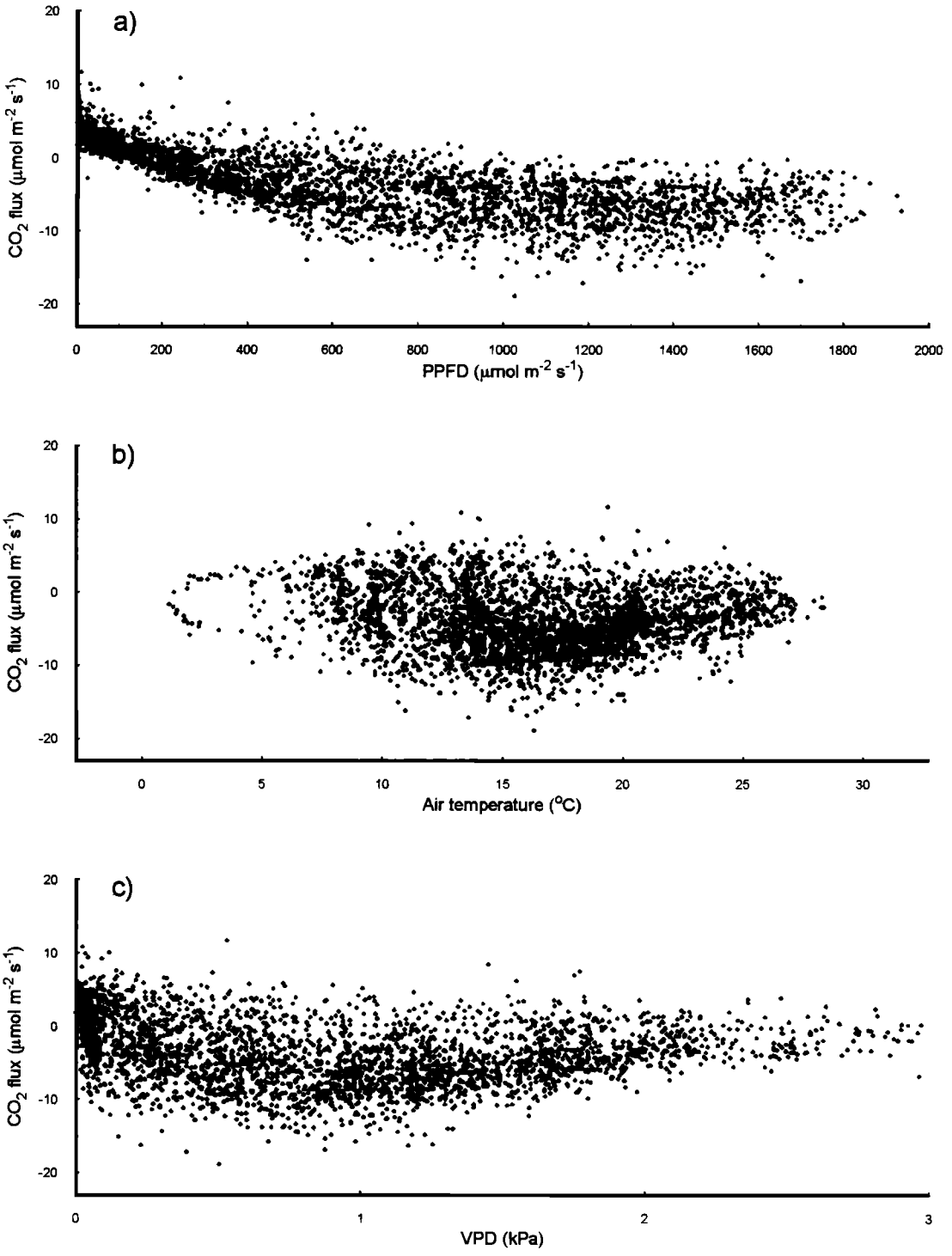

Figure 10. Half-hourly net ecosystem flux densities in relation to (a) incident PPFD, (b) air temperature, and (c) atmospheric vapor pressure deficit (VPD), at 27 m. Other details as given in Figure 3.

To determine the effect of increasing respiration with temperature on the apparent relationships in Figure 10, the assimilation of CO_2 in photosynthesis by the ecosystem (regarded as positive) has been calculated by adding the respiration rate, at the appropriate temperature, to the net ecosystem flux for each daytime, unstable half hour depicted in Figure 10. The respiration rate was derived from the nighttime CO_2 efflux in well-mixed conditions, as described earlier. The results of this in Figure 11 show an enhanced ecosystem response to PPFD, an increase in assimilation in relation to air temperature over the seasonal range, and little or no response of assimilation to VPD. Measurements of CO_2 assimilation rate of the trees alone made with the branch bags show an essentially similar response to PPFD but a sharper temperature optimum and a reduction in photosynthesis with increasing VPD (M. B. Rayment and P. G. Jarvis, manuscript in preparation, 1997). With the data presently available, we are not able to partition photosynthetic activity between the

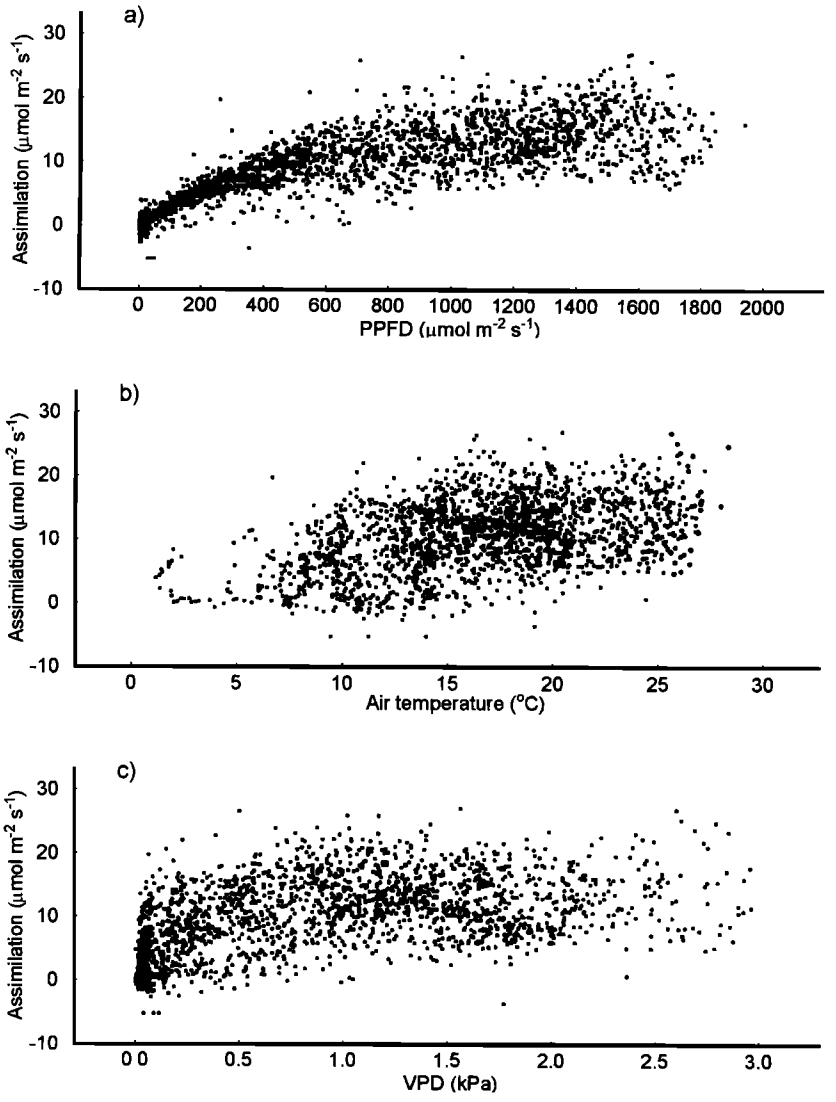

Figure 11. Half-hourly net CO_2 assimilation rates by all vegetation in relation to (a) incident PPFD, (b) air temperature, and (c) atmospheric VPD, at 27 m. Other details as given in Figure 3.

tree canopy, understory herbaceous ground vegetation, and moss layer.

Directional Net Ecosystem Biotic Flux

The largest average daytime net biotic flux (exceeding 6 μmol $m^{-2} s^{-1}$) occurred in the SE-SW sector of the site (Figure 12a). In this direction the CASI image shows the most extensive area of dense well-grown trees. By contrast, the largest number of observations occurred in the NW sector (Figure 12b).

This type of discrepancy has not so far been included in our analysis or, as far as we are aware, in anyone elses. We introduce it here to show a potential source of uncertainty in deriving the best area-averaged estimates of fluxes.

Seasonal Net Ecosystem Biotic Flux

The seasonal course of the net biotic flux integrated over 24 hours is shown in Figure 13. To obtain these daily totals, nighttime effluxes for stable nights with $u^* < 0.4$ m s^{-1} were modeled on the basis of the effluxes measured on unstable nights, as described earlier. The net effect of this has been to reduce the daily carbon gain integrated over the 120 day growing season from an initial estimate of 180 g m^{-2} to 95 g m^{-2}, a reduction to 56% of the initial value, and to increase the number of days with a net loss of carbon from 11 to 31. Figure 13 shows that the daily net ecosystem flux was already considerable at the start of IFC1 and that it fluctuated somewhat erratically through the season, ending with a general decline through IFC3, when the number of days with a net loss of carbon increased. It is evident from inspection of Figure 13 that these days were either days of low PPFD or days of high temperature, or a combination of both. Low PPFD results in low rates of CO_2 uptake in photosynthesis by the foliage of the whole ecosystem, as shown in Figure 11: high temperature results in high rates of CO_2 production in respiration, largely from the soil [*Rayment and Jarvis*, this issue].

The cumulated net ecosystem fluxes of water and carbon, taken from Figures 6 and 13, respectively, are shown in Figure 14. Over the 120 day period there was a net gain of 95 g m^{-2} of carbon in relation to evapotranspiration of 237 mm of water. Following the analysis of *Moncrieff et al.* [1996] and *Goulden et al.* [1996a], the sink strength for carbon should be quoted as

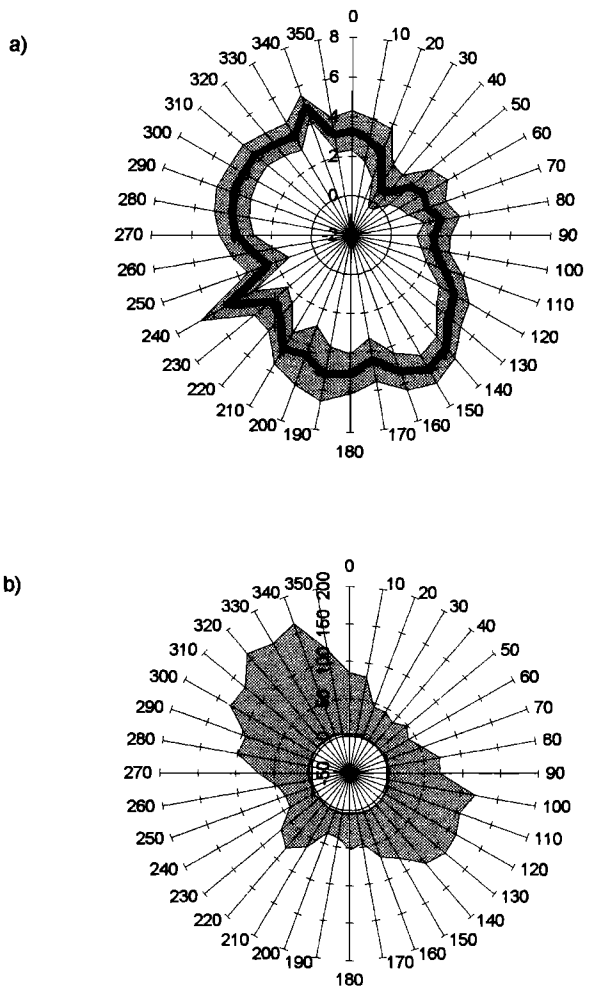

Figure 12. (a) Average biotic daylight net CO_2 fluxes with respect to direction around the tower. The units are μmol m^{-2} s^{-1}, and 360/0° is north. (b) The number of half-hour measurements with respect to direction around the tower. In both Figures 12a and 12b, the data plotted at the upper limit of the 10° interval to which they apply.

$0.95 \pm 0.01 \pm 0.2$ t ha^{-1}, where the first term in the uncertainty refers to random errors, and the second to systematic errors. Thus random errors pose little threat to the confidence with which we can say that the OBS was a sink, particularly because the longer the time period over which the measurements are made, the smaller is the uncertainty attached to the long-term average value. Additional systematic errors would have to be a factor of 5 larger to turn the OBS into a source of carbon rather than a sink, and we know of no phenomena or instrumental problems which could bring this about. Systematic errors, either full or selective, are unlikely to exceed ±20% [*Moncrieff et al.*, 1996], and the sink strength is unequivocal within these limits.

The period of measurements encompassed the major part of the growing season and, consequently, does not show the full annual range of seasonality, as was also the case on the neighboring, but sandy, jack pine site [*Baldocchi et al.*, this issue, 1997]. The results obtained on these two coniferous sites in the southern study area are broadly similar, but the jack pine site experienced water stress on three occasions, and this was particularly severe in July/August, when the Bowen ratios were much higher and the CO_2 fluxes much lower than on the black spruce site, which dried out only marginally in the 0–30 cm horizons during the latter part of August.

While cumulative evapotranspiration was continuing to rise at the end of the period, it is noticeable that the accumulation of carbon had leveled off. It is difficult to model the carbon balance over a full year on the basis of the 120 days of data because temperatures in the early spring, late fall, and winter lie outside the range encountered in the growing season over which these measurements were made. There would have been an additional gain of carbon in the spring, but Figure 13 suggests that losses of carbon may have continued to increase through the fall after the end of IFC3 until the freeze-up.

Conclusions

With respect to the two BOREAS objectives defined at the outset, there are two main conclusions. First, the evapotranspiration rates were lower, and the Bowen ratios higher, than

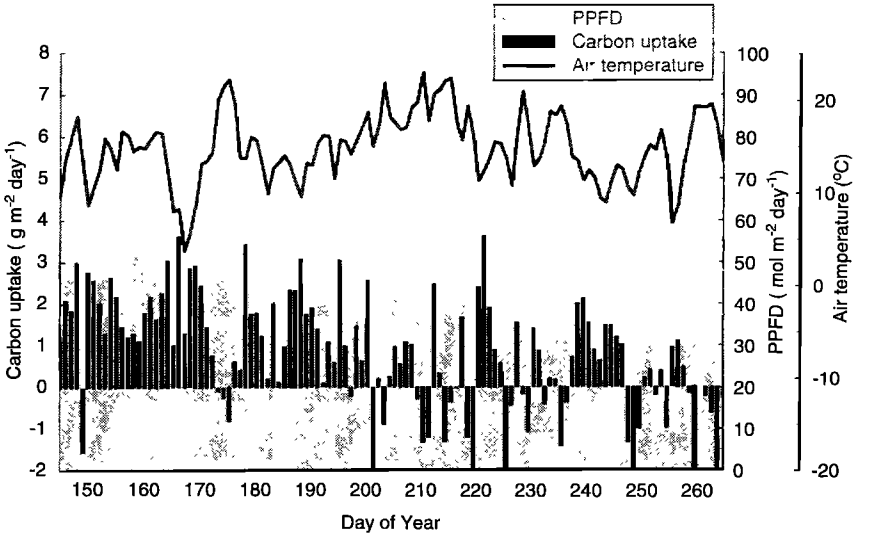

Figure 13. Seasonal course of daily integrated net ecosystem biotic CO_2 flux density and photosynthetic photon flux density for the 120 days from May 23 (day 143) to September 21 (day 264). Each column represents the total flux density integrated over 24 hours.

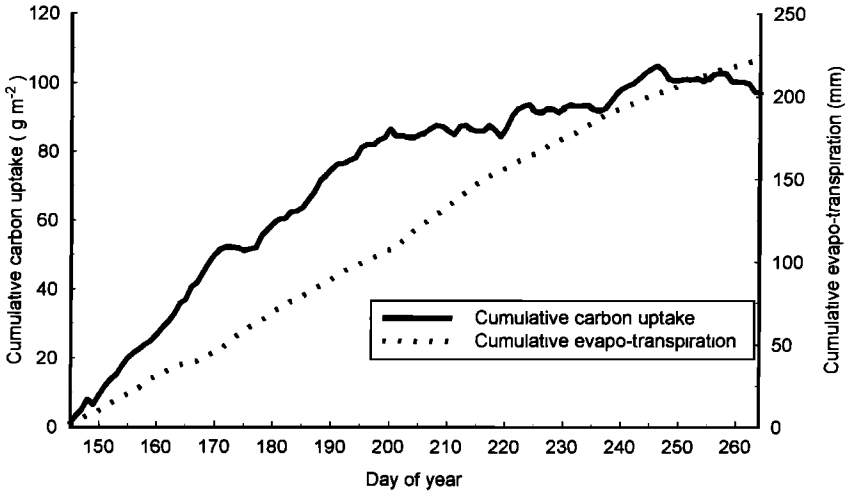

Figure 14. Cumulative evapotranspiration and net carbon gain for the period of 120 days from May 23 (day 143) to September 21 (day 264) in 1994. The data are taken from Figures 6 and 8, respectively. The daily average carbon and water flux densities over the period are 0.8 g m^{-2} and 2 mm, respectively.

anticipated, although compatible with earlier observations made over diverse spruce forests using flux-gradient methods [*Jarvis et al.*, 1976; *Jarvis*, 1994; *Ruimy et al.*, 1995]. A likely consequence of this is that the surface is warmer and the atmosphere drier than over prairie and croplands, and this may both generate a stronger forcing function and influence regional climate. Second, this old black spruce stand on the southern edge of the boreal forest was a significant carbon sink over the summer growing season and may well be a significant sink on an annual basis. In view of the large proportion of black spruce, much of it much younger, in the Canadian boreal forest zone, this carbon sink may make a significant contribution to the global carbon budget.

From a scientific perspective, two main questions have come to the fore. First, our understanding of the processes driving fluxes between forests and the atmosphere at night is inadequate, and additional information is needed from different methodologies to find out what is happening. The use of balloon ascents carrying tether-sondes through the inversion layer at night is likely to be a useful way of finding out if CO_2 is escaping upward at night without being measured by the eddy covariance sensor. Second, it is clear that measurements are needed in the spring, fall, and winter to enable an annual carbon budget to be calculated. By contrast with the tropics, the extreme seasonality of the boreal climate precludes making a reliable estimate using models parameterized with data from only part of the year. These issues were addressed in the 1996 campaign, and the data are now being analyzed.

Acknowledgments. The authors acknowledge the financial support provided by NERC through its Terrestrial Initiative in Global Environment Research (TIGER) program, awards GST/02/619 and GST/02/984. S.H. was supported by a Department of Education, Northern Ireland, Research Studentship. M.R. was supported by a NERC Studentship. We thank Tom Gower for providing data on the stand structure. We are grateful to Dennis Baldocchi and his colleagues for much productive discussion on our respective sites during this 1994 campaign and to Steve Wofsy and Mike Goulden for constructive criticism of the manuscript.

References

Baldocchi, D. D., C. A. Vogel, and B. Hall, Seasonal variation of carbon dioxide exchange rates above and below a boreal jack pine forest, *Agric. For. Meteorol.*, *83*, 147–170, 1997.

Baldocchi, D. D., C. A. Vogel, and B. Hall, Seasonal variation of energy and water vapor exchange rates above and below a boreal jack pine forest canopy, *J. Geophys. Res.*, this issue.

Chen, J. M., P. M. Rich, T. S. Gower, J. M. Norman, and S. Plummer, Leaf area index of boreal forests: Theory, techniques, and measurements, *J. Geophys. Res.*, this issue.

Ciais, P., P. P. Tans, M. Trolier, J. W. C. White, and R. J. Francey, A large northern terrestrial CO_2 sink indicated by the $^{13}C/^{12}C$ ratio of atmospheric CO_2, *Science*, *269*, 1098–1102, 1995.

Conway, T. C., P. P. Tans, L. S. Waterman, K. W. Thoning, D. R. Kitzis, K. A. Masarie, and N. Zhang, Evidence for interannual variability of the carbon cycle from the NOAA/CMDL global air sampling network, *J. Geophys. Res.*, *99*, 22,831–22,855, 1994.

Denmead, O. T., and E. F. Bradley, Eddy correlation measurement of the CO_2 flux in plant canopies, in *Proceedings, 4th Australasian Conference on Heat and Mass Transfer*, pp. 183–192, Secretariat, Fourth Australasian Conf. on Heat and Mass Transfer, Christchurch, N. Z., 1989.

Denning, A. S., I. Y. Fung, and D. Randall, Latitudinal gradient of atmospheric CO_2 due to seasonal exchange with land biota, *Nature*, *376*, 240–243, 1995.

Francey, R. J., P. P. Tans, C. E. Allison, I. G. Enting, J. W. C. White, and M. Trolier, Changes in oceanic and terrestrial carbon uptake since 1982, *Nature*, *373*, 326–330, 1995.

Goulden, M. L., J. W. Munger, S.-M. Fan, B. C. Daube, and S. C. Wofsy, Measurements of carbon sequestration by long-term eddy covariance: Methods and a critical evaluation of accuracy, *Global Change Biol.*, *2*, 169–182, 1996a.

Goulden, M. L., J. W. Munger, S.-M. Fan, B. C. Daube, and S. C. Wofsy, Exchange of carbon dioxide by a deciduous forest: Response to interannual climate variability, *Science*, *271*, 1576–1578, 1996b.

Grace, J., Y. Malhi, J. Lloyd, J. McIntyre, A. C. Miranda, P. Meir, and H. Miranda, The use of eddy covariance to infer the carbon balance of Brazilian rain forest, *Global Change Biol.*, *2*, 209–218, 1996.

Jarvis, P. G., Capture of carbon dioxide by a coniferous forest, in *Resource Capture by Crops*, edited by J. L. Monteith, R. K. Scott, and M. H. Unsworth, pp. 351–374, Nottingham Univ. Press, Nottingham, England, 1994.

Jarvis, P. G., G. B. James, and J. J. Landsberg, Coniferous forest, in *Vegetation and the Atmosphere*, vol. 2, edited by J. L. Monteith, pp. 171–240, Academic, San Diego, Calif., 1976.

Keeling, R. F., S. C. Piper, and M. Heimann, Global and hemispheric

CO_2 sinks deduced from changes in atmospheric O_2 concentration, *Nature*, *381*, 218–221, 1996.

Leuning, R. L., and M. J. Judd, The relative merits of open- and closed-path analysers for measurement of eddy fluxes, *Global Change Biol.*, *2*, 241–254, 1996.

Moncrieff, J. B., Y. Malhi, and R. Leuning, The propagation of errors in long-term measurements of land atmosphere fluxes of carbon and water, *Global Change Biol.*, *2*, 231–240, 1996.

Moncrieff, J. B., J. M. Massheder, A. Verhoef, J. Elbers, B. H. Heutsunkveld, S. Scott, H. de Bruin, P. Kabat, H. Soegaard, and P. G. Jarvis, A system to measure surface fluxes of energy, momentum and carbon dioxide, *J. Hydrol.*, *188–189*, 589–611, 1997.

Monteith, J. L., Evaporation and environment, in *The State and Movement of Water in Living Organisms*, *Symp. Soc. Exp. Biol.*, vol. 19, pp. 205–234, Cambridge Univ. Press, New York, 1965.

Ogunjemiyo, O. S., P. H. Schuepp, J. I. MacPherson, and R. L. Desjardins, Analysis of flux maps versus surface characteristics from Twin Otter grid flights in BOREAS 1994, *J. Geophys. Res.*, this issue.

Rayment, M. B., and P. G. Jarvis, An improved open chamber system for measuring soil CO_2 effluxes in the field, *J. Geophys. Res.*, this issue.

Ruimy, A., P. G. Jarvis, D. D. Baldocchi, B. Saugier, and R. Valentini, CO_2 fluxes over plant canopies: A review, in *Advances in Ecological Research*, vol. 26, edited by M. Begon and A. H. Fitter, pp. 2–68, Academic, San Diego, Calif., 1995.

Sellers, P., et al., The Boreal Ecosystem-Atmosphere Study (BOREAS): An overview and early results from the 1994 field year, *Bull. Am. Meteorol. Soc.*, *76*, 1549–1577, 1995.

Webb, E. K., G. I. Pearman, and R. Leuning, Correction of flux measurements for density effects due to heat and water vapour transfer, *Q. J. R. Meteorol. Soc.*, *106*, 85–100, 1980.

Wofsy, S. C., M. L. Goulden, J. W. Munger, S.-M. Fan, P. S. Bakwin, B. C. Daube, S. L. Bassow, and F. A. Bazzaz, Net exchange of CO_2 in a mid-latitude forest, *Science*, *260*, 1314–1317, 1993.

S. E. Hale, P. G. Jarvis, J. M. Massheder, J. B. Moncrieff, M. Rayment, and S. L. Scott, Institute of Ecology and Resource Management, University of Edinburgh, Darwin Building, Mayfield Road, Edinburgh EH9 3JU, Scotland, United Kingdom. (e-mail: p.jarvis@ed.ac.uk)

(Received August 27, 1996; revised March 24, 1997; accepted March 26, 1997.)